# The Role of Glu 57 in the Mechanism of the *Escherichia coli* MutT Enzyme by Mutagenesis and Heteronuclear NMR†

Jian Lin,‡ Chitrananda Abeygunawardana,‡ David N. Frick,§ Maurice J. Bessman,§ and Albert S. Mildvan*,‡

*Department of Biological Chemistry, The Johns Hopkins School of Medicine, 725 North Wolfe Street, Baltimore, Maryland 21205-2185, and Department of Biology, The Johns Hopkins University, Charles and 34th Streets, Baltimore, Maryland 21218*

*Received December 28, 1995; Revised Manuscript Received March 19, 1996*⊗

ABSTRACT: The role of the conserved residue Glu-57 in the mechanism of the MutT enzyme from *Escherichia coli* was investigated by mutagenesis and heteronuclear NMR methods. The enzymatic activity of the E57Q mutant is at least $10^5$-fold lower than that of the wild type enzyme. The solution structure of the E57Q mutant, based on comparisons of $^1H-^{15}N$ NOESY HSQC spectra and $^1H-^{15}N$ HSQC spectra to those of the wild type enzyme, differs in a region near Glu-57. The dissociation constants ($K_D$) of the E-$Mg^{2+}$ and E-$Mn^{2+}$ complexes increased 3.3- and 3.6-fold, respectively, in the E57Q mutant, while the $K_D$ of E-dGTP is unaltered from that of the wild type enzyme. The enhanced paramagnetic effect of enzyme-bound $Mn^{2+}$ on $1/T_1$ of water protons is halved in the E57Q mutant indicating an altered metal-binding site. $^1H-^{15}N$ HSQC titrations of E57Q with $MnCl_2$ show selective attenuation of the side chain NH signals of Gln-57 and the backbone NH signals of Gly-37, Gly-38, Lys-39, Glu-53, Glu-56, Gln-57, and Glu-98, indicating proximity of bound $Mn^{2+}$ to these residues. The same resonances of the wild type and the E57Q mutant enzymes are attenuated by $Mn^{2+}$, but significantly smaller paramagnetic effects (relative to the largest effect on Lys-39) are found on Gly-37, Gly-38, Val-58, and Glu-98 of the mutant, indicating an altered position of the bound divalent cation. Thus Glu-57 is probably a ligand to the enzyme-bound metal, and the profound loss of catalytic activity in the E57Q mutant results from structural and electronic changes at the site of the enzyme-bound divalent cation. $^1H-^{15}N$ HSQC titrations of the wild type enzyme with $MgCl_2$ show changes in chemical shifts of $^{15}N$ and NH resonances in regions closely overlapping those induced by the E57Q mutation itself, suggesting that the loss of the negative charge at Glu-57, either by mutation or by neutralization with $Mg^{2+}$, induces a similar effect. In the E57Q mutant, the slow exchange of the side chain $NH_2$ protons of Gln-57 and NOE's from the $NH_2$ protons of Gln-57 to the $\beta$ and $\gamma$ protons of Glu-98 suggests hydrogen bonding of Gln-57 to Glu-98 in the free enzyme. $^1H-^{15}N$ HSQC titrations of both the wild type and mutant enzymes with dGTP show changes in $^{15}N$ and NH chemical shifts of residues in a cleft formed by $\beta$-strands A, C, and D on one side and loop I, the end of loop IV, and the beginning of helix II on the other side, suggesting this cleft to be the nucleotide binding site. These changes in chemical shift were smaller or absent in titrations of the wild type or mutant enzymes with AMPCPP or $Mg^{2+}$-AMPCPP, in accord with the strong preference of the MutT enzyme for guanine over adenine nucleotide substrates.

The MutT enzyme from *Escherichia coli*, a pyrophosphohydrolase of 129 residues, catalyzes the unusual hydrolysis of nucleoside and deoxynucleoside triphosphates (NTP) by nucleophilic substitution at the rarely attacked $\beta$-phosphorus, yielding pyrophosphate and a nucleotide (NMP) as products (Bhatnagar *et al*., 1991; Weber *et al*., 1992). Like other enzymes which catalyze substitution at the electron-rich $\beta$-phosphorus, this enzyme requires two divalent cations for activity and forms a MutT-$M^{2+}$−NTP-$M^{2+}$ complex (Frick *et al*., 1994). The biological role of this enzyme in preventing mutations is linked to its enzymatic activity (Mejean *et al*., 1994) by preferentially hydrolyzing nucleotides which could be misincorporated during DNA replication, thus "sanitizing" the nucleotide pool (Bhatnagar *et al*., 1991, and references therein). MutT is one of a class of enzymes which specifically prevents AT → CG transversions, thereby decreasing the mutation rate in bacteria by several orders of magnitude (Kamath & Yanofsky, 1993; Mejean *et al*., 1994). Maki and Sekiguchi (1992) have proposed that the biological substrate of the MutT enzyme is 8-oxo-dGTP, an oxidatively modified nucleotide which can mispair with template adenine during DNA synthesis *in vitro* (Cheng *et al*., 1991). An enzyme similar to *E. coli* MutT has been characterized from a human cell line (Mo *et al*., 1992; Sakumi *et al*., 1993).

Heteronuclear NMR[1] studies of MutT have shown the solution secondary structure to consist of a five-stranded

† This work was supported in part by National Institutes of Health Grants DK28616 (to A.S.M.) and GM18649 (to M.J.B).

* To whom correspondence should be addressed. Phone: (410) 955-2038. FAX: (410) 955-5759.

‡ The Johns Hopkins School of Medicine.

§ The Johns Hopkins University.

⊗ Abstract published in *Advance ACS Abstracts,* May 1, 1996.

[1] Abbreviations: AMPCPP, $\alpha,\beta$-methyleneadenosine triphosphate; 8-azido ATP, 8-azidoadenosine triphosphate; FID, free induction decay; HSQC, heteronuclear single-quantum correlation; NMR, nuclear magnetic resonance; NOE, nuclear Overhauser effect; NOESY, nuclear Overhauser effect spectroscopy; 2D, two-dimensional; 3D, three-dimensional; TOCSY, total correlation spectroscopy; TPPI, time-proportional phase incrementation; TSP, sodium 3-(trimethylsilyl)-propionate-2,2,3,3-$d_4$.

S0006-2960(95)03071-6 CCC: $12.00 

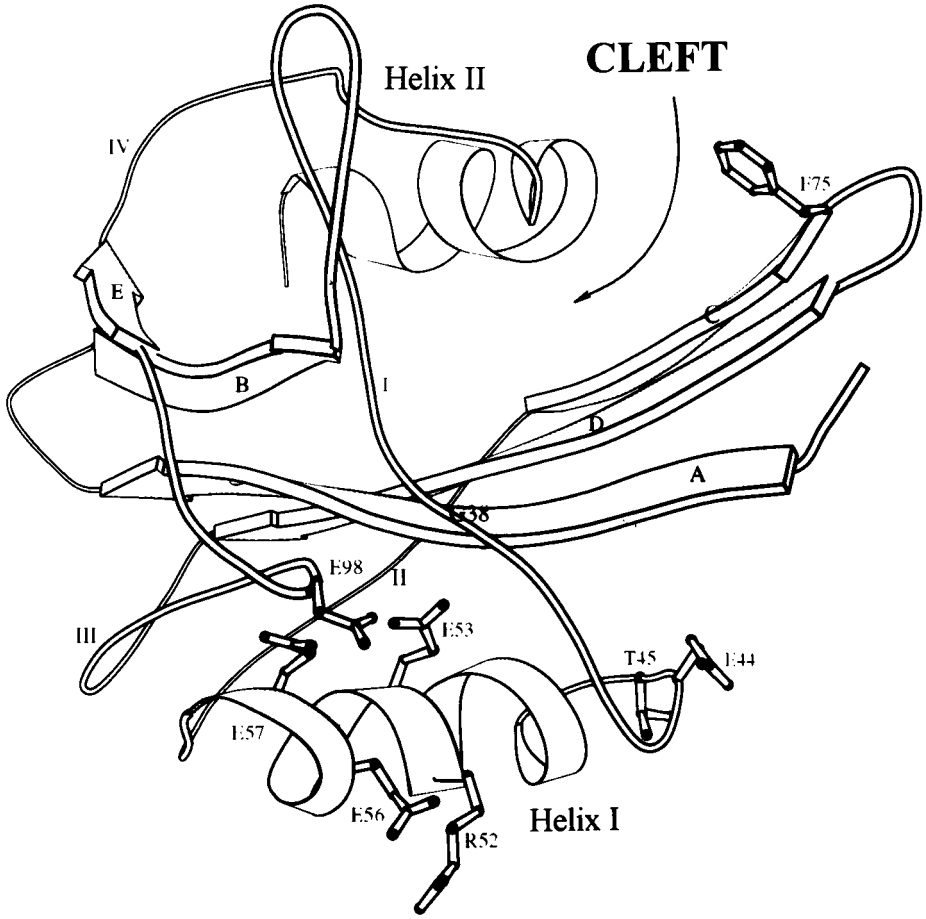


FIGURE 1: Solution structure of the free MutT enzyme of lowest van der Waals energy (Abeygunawardana *et al*., 1995). MOLSCRIPT diagram (Kraulis, 1991) showing residues conserved among related nucleoside triphosphate pyrophosphohydrolases. Also labeled are the secondary structural elements and the cleft.

mixed $\beta$-sheet connected by the loop I−α-helix I−loop II motif, by two tight turns, and by loop III and terminated by loop IV−α helix II (Abeygunawardana *et al*., 1993; Weber *et al*., 1993). The tertiary structure (see Figure 1) (Abeygunawardana *et al*., 1995) is globular and compact, with the parallel portion of the $\beta$-sheet sandwiched between the two α-helices, forming an α+$\beta$ fold. A cluster of four conserved glutamate residues (53, 56, 57, and 98) forms a patch of strongly negative electrostatic potential in the three-dimensional structure.

Previous experiments have shown the backbone NH of Glu-57 to be near one or both of the $Mn^{2+}$ binding sites in the MutT-$Mn^{2+}$−AMPCPP-$Mn^{2+}$ complex, based on selective paramagnetic effects in the $^{1}H-^{15}N$ HSQC spectrum (Frick *et al*., 1995b). Because Glu-57 is conserved among MutT-like enzymes (Figure 1), and because of its proximity to one or both of the divalent cation binding sites, the effects of mutating this residue to Gln were studied. A preliminary report of this work has been published (Lin *et al*., 1995).

## MATERIALS AND METHODS

*Preparation of E57Q E. coli MutT Mutant by Site-Directed Mutagenesis*. The megaprimer method of Sarkar and Sommer (1990) as modified by Barik (1993) was used to make the E57Q mutant of the MutT enzyme. Plasmid pETMutT was used as the template for a polymerase chain reaction with a primer (5′-AAT CCC GAC TTG TTC CTG AAG-3′) complementary to the coding strand containing the appropriate mispair (underlined) in the codon designating amino acid Glu-57, and a second primer upstream of the MutT gene. The resulting DNA product was isolated from an agarose gel, purified, and used in second polymerase chain reaction as a "megaprimer" with a primer downstream from the MutT gene and the plasmid pETMutT as the template. The resulting product contained the altered MutT gene between *Xb*I and *Bam*HI restriction sites. The DNA was purified by agarose gel electrophoresis, digested with the appropriate restriction enzymes, and ligated into the digested plasmid vector pET11b. The resulting plasmid pETE57Q was transformed into strain HB101 for storage and into strain BL21 (DE3) for protein expression. Plasmids pETE57Q were sequenced to confirm that the amino acid codon substitution at position 57 was the only change.

*Protein Sample Preparation*. Uniformly $^{15}N$-enriched $^{15}NH_4Cl$ (99% $^{15}N$) was purchased from Cambridge Isotope Labs (Woburn, MA). The wild type and E57Q mutant MutT proteins labeled with $^{15}N$ were expressed and purified to homogeneity as previously described (Abeygunawardana *et al*., 1993).

*MutT Enzyme dGTPase Assay*. The activities of the wild type and E57Q mutant enzymes were determined by the most sensitive assay reported which directly measures the appearance of [$^{32}P$]pyrophosphate released from [$\gamma$-$^{32}P$]-labeled dGTP (Bhatnagar *et al*., 1991).

*General Heteronuclear NMR Methods*. Unless otherwise noted, solution conditions for structural NMR studies were 0.75 mM labeled MutT, 6 mM $d_{11}$-Tris-HCl, in 0.65 mL of $H_2O/^2H_2O$ (90:10) at pH 7.5 and at 32 °C. The NMR data were collected on a Varian Unityplus 600 NMR spectrometer and transferred to a Silicon Graphics Personal IRIS 4D/35

Work Station for processing and analysis with the FELIX software package (Biosym Technologies, Inc.). Unless otherwise noted, multidimensional data sets were collected using the States-TPPI method (Marion *et al*., 1989) in all of the indirect dimensions, with relaxation delays of 1 s. These acquired time domain data points were extended by one-third of the original size by the forward linear prediction routine in FELIX, before further processing to yield the final frequency domain data. The observed $^1$H chemical shifts are reported with respect to the $H_2O$ or $HO^2H$ signal, which is taken as 4.706 ppm downfield from external TSP at 32 °C. The nitrogen chemical shifts are reported with respect to external $^{15}NH_4Cl$ (2.9 mM in 1 M HCl) at 20 °C, which is 24.93 ppm downfield from liquid $NH_3$ (Levy & Lichter, 1979).

*3D $^1$H−$^{15}$N NOESY-HSQC and 3D $^1$H−$^{15}$N TOCSY-HSQC Spectra of E57Q MutT Mutant*. A 3D $^1$H−$^{15}$N NOESY-HSQC experiment was recorded on a 1.3 mM solution of $^{15}$N-labeled MutT (E57Q mutant) containing the other components as described above, with a 150 ms mixing time using a pulse sequence in which the HSQC detection scheme was optimized to avoid water saturation (Mori *et al*., 1995). The data were obtained at 600 MHz with spectral widths of 6960, 1824, and 8200 Hz in $f_1$ ($^1$H), $f_2$ ($^{15}$N), and $f_3$ ($^1$HN), respectively, and with 128, 36, and 512 complex points, respectively, in the $t_1$, $t_2$, and $t_3$ dimensions. A total of four transients were acquired for each hypercomplex $t_1$, $t_2$ pair, requiring 26 h to accumulate the data. The final data matrix was 512 × 128 × 512 real points for the $f_1$ ($^1$H), $f_2$ ($^{15}$N), and $f_3$ ($^1$HN) dimensions, respectively.

A 3D $^1$H−$^{15}$N TOCSY-HSQC experiment was recorded on the same sample using the pulse sequence of Zhang *et al*. (1994) and a mixing time of 28 ms. The data were obtained at 600 MHz with spectral widths of 6960, 1824, and 8200 Hz in $f_1$ ($^1$H), $f_2$ ($^{15}$N), and $f_3$ ($^1$HN), respectively, and with 92, 36, and 512 complex points respectively in the $t_1$, $t_2$, and $t_3$ dimensions for a total time of 18 h. A total of eight transients were acquired for each hypercomplex $t_1$, $t_2$ pair. The final data matrix was 512 × 128 × 512 real points for the $f_1$ ($^1$H), $f_2$ ($^{15}$N), and $f_3$ ($^1$HN) dimensions, respectively.

*$^1$H−$^{15}$N HSQC Spectra of E57Q Mutant and Wild Type Enzymes*. $^1$H−$^{15}$N HSQC spectra were recorded at enzyme concentrations of 0.75 mM in samples containing the other components as described above, using the fast HSQC sequence of Mori *et al*. (1995). The data were acquired with spectral widths of 1946 and 10 000 Hz in $f_1$ ($^{15}$N) and $f_2$ ($^1$H), respectively, and with 512 and 2560 complex points, respectively, in the $t_1$, and $t_2$ dimensions. A total of eight transients were acquired for each hypercomplex $t_1$ point with $^1$H and $^{15}$N carriers positioned at 4.71 and 43 ppm, respectively, requiring 45 min to collect the data. The final data matrix was 1024 × 1024 real points for the $f_1$ ($^{15}$N) and $f_2$ ($^1$H) dimensions, respectively.

*$^1$H−$^{15}$N HSQC Titrations of E57Q and Wild Type Enzymes*. In titrations of MutT (0.75 mM) with $Mn^{2+}$, $MnCl_2$ was added stepwise to the enzyme solution and the $^1$H−$^{15}$N HSQC spectra were recorded. For the wild type enzyme the concentrations of $Mn^{2+}$ in each of the titration steps were 0, 2, 4, 6, 9, 12, 15, and 18 $\mu$M. For the E57Q mutant the total concentrations of $Mn^{2+}$ in each titration were 0, 4, 8, 16, 24, 32, 40, 48, 56, and 64 $\mu$M. At each concentration of $Mn^{2+}$, the intensity of the cross-peaks were measured by volume integration using the FELIX software package.

In other titrations, $MgCl_2$ or dGTP was added stepwise to MutT solutions (0.75 mM) and $^1$H−$^{15}$N HSQC spectra were recorded. For the wild type enzyme, the concentrations of $Mg^{2+}$ in the titrations were 0, 0.375, 0.75, 1.5, and 3.0 mM. For the E57Q mutant, the concentrations of $Mg^{2+}$ were 0, 0.1, 0.2, 0.4, 0.75, 1.5, 3.0, and 6.0 mM. For both the wild type and the E57Q mutant enzymes, the concentrations of dGTP in the titrations were 0, 0.375, 0.75, 1.5, 3.0, and 4.5 mM.

After data processing, the resonances which showed the largest chemical shift change in either the $^1$H or $^{15}$N dimension were chosen and the change in chemical shift ($\Delta\delta$) was plotted against the concentration of either $Mg^{2+}$ or dGTP. Fitting the titration curves with eq 1 provided the dissociation constant ($K_D$) of either $Mg^{2+}$ or dGTP from the enzyme and the chemical shift difference ($\Delta\delta^\infty$) between the saturated binary complexes and that of the free enzyme for each resonance.

$$\Delta\delta = \Delta\delta^\infty((K_D + [L]_T + [E]_T) - \sqrt{((K_D + [L]_T + [E]_T)^2 - 4[L]_T[E_T])})/2[E]_T \quad (1)$$

In eq 1, $[L]_T$ is the total concentration of metal or substrate at each titration step and $[E]_T$ is the total concentration of enzyme.

*$^1$H−$^{15}$N HSQC Titration of Higher Complexes of the E57Q and Wild Type Enzymes*. To determine the interactions of the E57Q mutant enzyme with both metal and substrate, three $^1$H−$^{15}$N HSQC titrations were carried out. In the first, equimolar dGTP and $MgCl_2$ were added at concentrations of 0, 0.375, 0.75, 1.5, and 3.0 mM to a solution containing 0.75 mM mutant enzyme and 6 mM $MgCl_2$. Other components and conditions were as described above. Under these conditions, at least 99% of the dGTP was present as $Mg^{2+}$-dGTP. In the second titration, $MgCl_2$ at concentrations of 0, 5.25, 6.0, 7.5, and 10.5 mM was added to a solution containing 0.75 mM mutant enzyme and 4.5 mM dGTP. The third titration made use of the nonhydrolyzable nucleotide AMPCPP. A solution containing 0.75 mM mutant enzyme and 6.0 mM $MgCl_2$ was titrated with equimolar $MgCl_2$ and AMPCPP at concentrations of 0, 1.5, 3.0, 4.5, and 6.0 mM. For the wild type enzyme, because of its high catalytic activity, only the third type of titration was possible. A solution containing 0.75 mM wild type enzyme and 3.0 mM $MgCl_2$ was titrated with equimolar $MgCl_2$ and AMPCPP at concentrations of 0, 0.75, 1.5, 3.0, and 6.0 mM. Under these conditions, at least 98% of the AMPCPP was present as its $Mg^{2+}$ complex.

The titration data were analyzed to obtain the dissociation constants of the higher complexes of MutT which have been defined as follows (Frick *et al*., 1994).

$$K_6 = [EM][GM]/[EMGM] \quad (2)$$

$$K_{11} = [M][EGM]/[EMGM] \quad (3)$$

$$K_{12} = [E][GM]/[EGM] \quad (4)$$

where [E], [GM], [M], [EM], [EGM], and [EMGM] are the concentrations of free enzyme, $Mg^{2+}$-dGTP, $Mg^{2+}$, enzyme-$Mg^{2+}$, enzyme-dGTP-$Mg^{2+}$, and enzyme-$Mg^{2+}$−dGTP-$Mg^{2+}$, respectively. The values of $K_6$, $K_{11}$, and $K_{12}$ were obtained by computing the concentrations of these six species from the changes in $^{15}$N chemical shifts ($\Delta\delta$) observed in

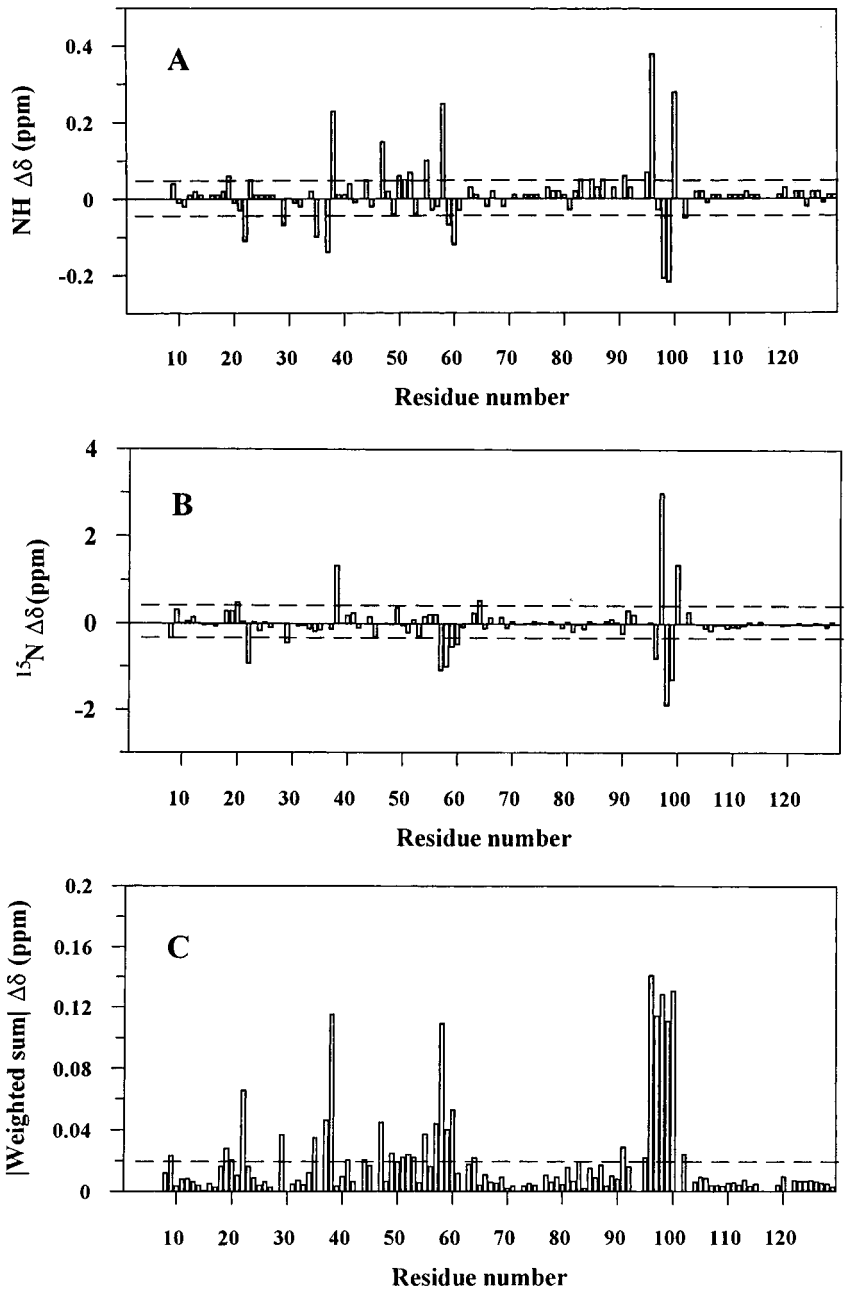


FIGURE 2: Backbone $^{15}$N and NH chemical shift differences between the E57Q mutant and wild type MutT enzymes. Chemical shift differences were calculated on the basis of the chemical shift values obtained from $^{1}$H−$^{15}$N HSQC spectra and plotted versus the residue number. Upper panel, NH chemical shift differences. Middle panel, $^{15}$N chemical shift differences. Lower panel, sum of the absolute magnitudes of the NH and $^{15}$N chemical shift changes which were weighted according to the backbone amide chemical shift dispersion in the $^{1}$H and $^{15}$N dimensions (3.37 and 28.41 ppm, respectively). The dashed lines indicate the error limits.

the HSQC titrations, making use of the conservation equations,

$$[GM]_T = [GM] + [EGM] + [EMGM] \quad (5)$$

$$[E]_T = [E] + [EM] + [EGM] + [EMGM] \quad (6)$$

$$[M]_T = 2[EMGM] + [M] + [EM] \quad (7)$$

where $[GM]_T$, $[E]_T$, and $[M]_T$, are the total concentrations of $Mg^{2+}$-dGTP, enzyme, and $Mg^{2+}$, respectively, and the binary dissociation constant is

$$K_2 = [E][M]/[EM] \quad (8)$$

which was measured separately. Experimentally, it was observed that the chemical shift of the backbone NH of Lys-97 is sensitive only to the occupancy of the enzyme bound metal site and the end point of the $^{15}$N chemical shift of both binary, and higher complexes ($\Delta\delta^{\infty}$) are nearly identical. The $^{15}$N chemical shift of the side chain $NH_2$ of Asn-119 is sensitive only to dGTP binding and the end point is also nearly identical in both binary and higher complexes. Hence, each concentration of titrant yielded at least two $\Delta\delta$ values, reflecting the composition of the system as follows:

$$\Delta\delta_{N119s1} = \Delta\delta^{\infty}{}_{N119s1}([EMGM] + [EGM])/[E]_T \quad (9)$$

$$\Delta\delta_{K97} = \Delta\delta^{\infty}{}_{K97}([EMGM] + [EM])/[E]_T \quad (10)$$

where $\Delta\delta_{N119s1}$ and $\Delta\delta_{K97}$ are the $^{15}$N chemical shift changes in each titration step for the side chain of Asn-119 and the backbone of Lys-97, respectively, and $\Delta\delta^{\infty}{}_{N119s1}$ and $\Delta\delta^{\infty}{}_{K97}$

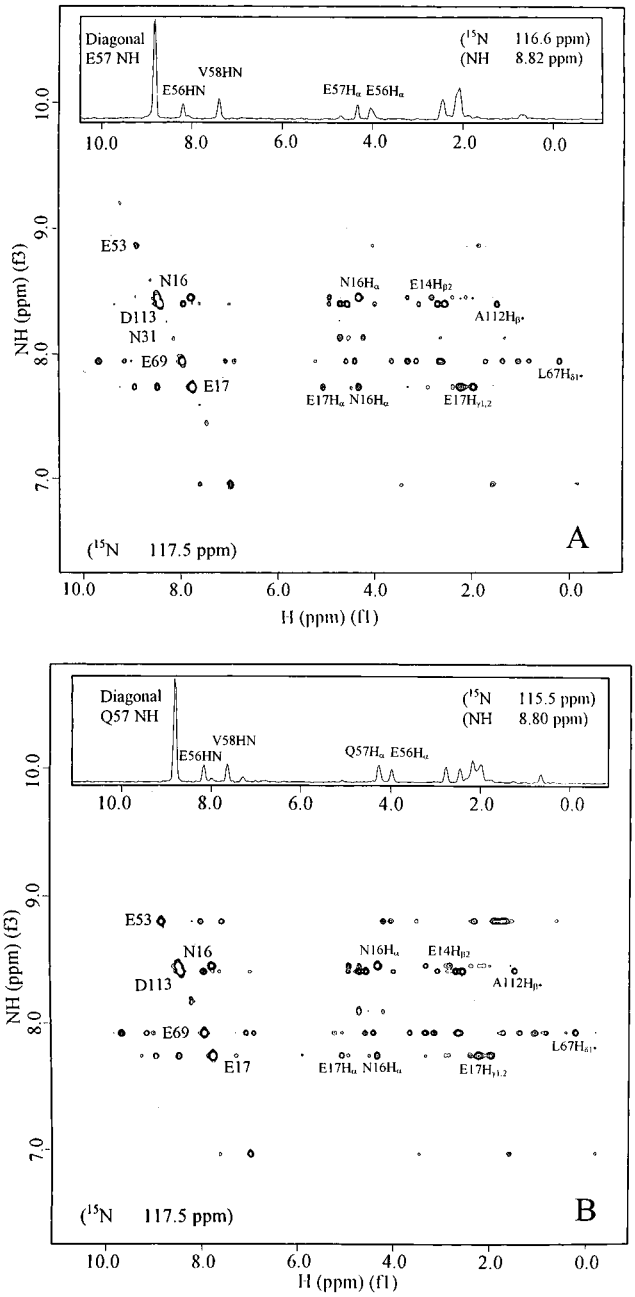


FIGURE 3: Comparison of the 3D $^1$H−$^{15}$N NOESY spectra of wild type and the E57Q mutant of MutT. (A) Selected $^1$H−$^1$H ($^{15}$N) plane (117.52 ppm) in the 600 MHz 3D $^1$H−$^{15}$N NOESY-HSQC spectrum of wild type MutT (0.75 mM) in $H_2O$ together with a 1D slice through the backbone NH resonance of Glu 57 (inset). (B) Selected $^1$H−$^1$H ($^{15}$N) plane (117.52 ppm) in the 600 MHz 3D $^1$H−$^{15}$N NOESY-HSQC spectrum of the E57Q mutant enzyme (1.30 mM) in $H_2O$ together with a 1D slice through the backbone NH resonance of Gln 57 (inset).

are the end points of these changes which were measured separately. Therefore each titration yielded a total of eight data points which were fit to eqs 5−10 to compute the concentrations of the six species [E], [GM], [M], [EM], [EGM], and [EMGM] from which the dissociation constants $K_6$, $K_{11}$, and $K_{12}$ were calculated at each point in the titration curve. These calculated values of $K_6$, $K_{11}$, and $K_{12}$ showed no drift with titrant concentration and were constant within their experimental errors of ≤15%.

*$Mn^{2+}$ Binding to the E57Q Mutant Enzyme*. The dissociation constant $K_2$ of the binary enzyme-$Mn^{2+}$ complex was determined by EPR which directly measures the concentration of free $Mn^{2+}$ in a mixture of free and enzyme-bound

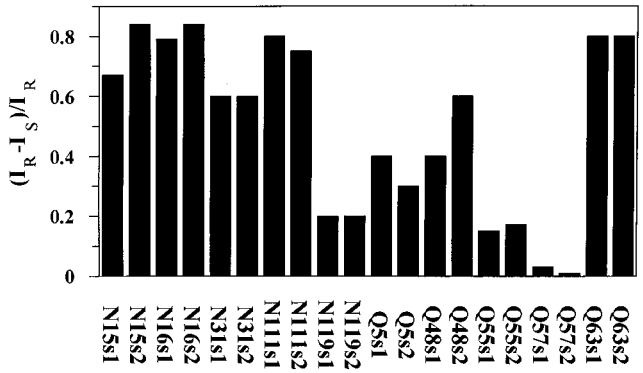


FIGURE 4: Water exchange behavior of side chain $NH_2$ groups of Asn and Gln residues in the E57Q mutant of MutT. Relative loss of NH peak intensities of the side chain $NH_2$ resonances of Asn and Gln residues in a $^1$H−$^{15}$N HSQC saturation transfer experiment on the E57Q mutant. $I_S$ is the intensity of the $NH_2$ signal in the HSQC spectrum with pre-saturation of water for 2.0 s using a 50 Hz radio frequency field, and $I_R$ is the intensity of the corresponding $NH_2$ signal in the HSQC spectrum with pre-irradiation at the control frequency of −5.30 ppm. The two side chain NH's were denoted as s1 and s2, respectively.

$Mn^{2+}$ (Cohn & Townsend, 1954) using a Varian E-4 EPR spectrometer. The concentration of enzyme was 464 $\mu$M, and that of $MnCl_2$ ranged from 112 to 1027 $\mu$M. The solutions also contained 50 mM Tris-HCl, pH 7.5, and the temperature was 22 °C. The EPR data were analyzed by Scatchard plots as previously described for the wild type enzyme (Frick *et al*., 1994). The enhanced paramagnetic effect of enzyme-bound $Mn^{2+}$ on the longitudinal relaxation rate ($1/T_1$) of water protons was measured at 24.3 MHz for the E57Q mutant, and the enhancement factor ($\epsilon_b$) was calculated as previously described for the wild type enzyme, correcting for the concentration of free $Mn^{2+}$ which was independently determined by EPR (Frick *et al*., 1994). The solutions and conditions were identical to those used for the EPR studies.

## RESULTS

*Kinetic Properties of the E57Q Mutant Compared with Wild Type MutT*. No catalytic activity of the highly purified E57Q mutant of MutT was detected using three assays of progressively increasing sensitivity: a colorimetric assay (Bhatnagar *et al*., 1991), an NMR assay (Weber *et al*., 1992), and a radioactivity assay (Bhatnagar *et al*., 1991; see Materials and Methods). The most sensitive radioactivity assay revealed the E57Q mutant to be at least $10^5$-fold less active than the wild type enzyme over a range of pH values from 6.0 to 10.0.

*Structural Properties of the E57Q Mutant Enzyme*. The profound loss of catalytic activity required a detailed study of the structure of the E57Q mutant to determine whether the protein had properly folded. $^1$H−$^{15}$N HSQC spectra of the E57Q mutant enzyme indicate that 84% of the backbone NH resonances are unshifted (i.e., are within 0.05 ppm of those of the wild type enzyme) and 62% of the backbone $^{15}$N resonances are unshifted (i.e., are within 0.1 ppm of those of the wild type enzyme) (Figure 2). The altered chemical shifts are given in the supplementary table (see supporting information). A 3D $^1$H−$^{15}$N TOCSY-HSQC spectrum of the E57Q mutant (not shown) which provided the $H_\alpha$ and $H_\beta$ assignments of most residues, revealed that 86% of the $H_\alpha$ and $H_\beta$ chemical shifts of the mutant are within 0.05 ppm of those of the wild type enzyme, suggesting a largely intact structure.

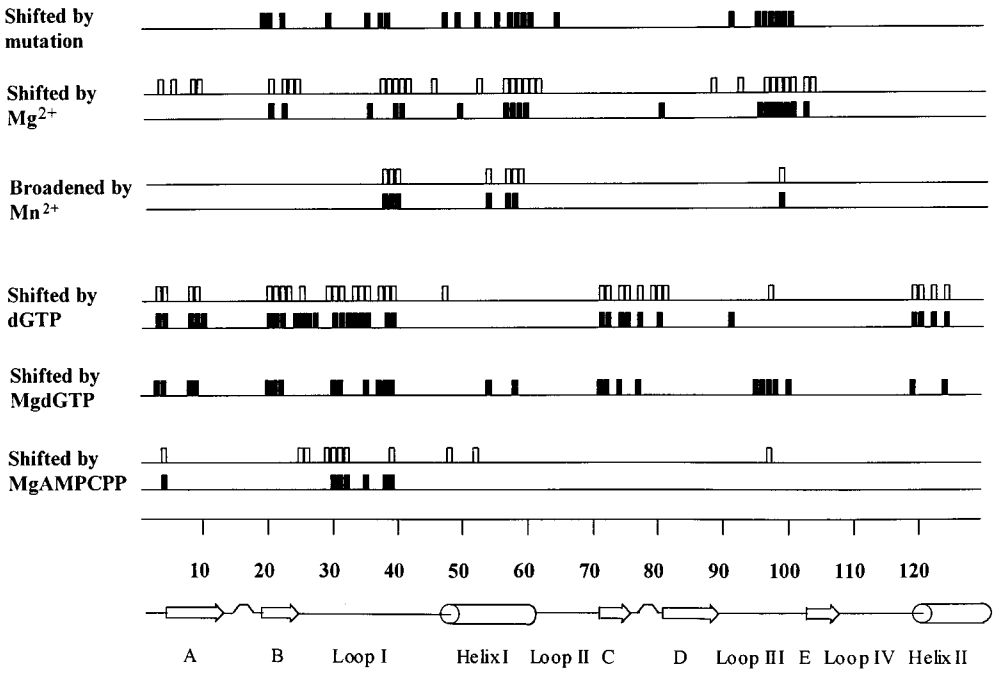


FIGURE 5: Summary of the effects of the E57Q mutation, metal, and substrate binding on the backbone $^{15}N$ and NH resonances of the MutT enzyme as a function of residue number and secondary structure. Open symbols are measured on the wild type enzyme, and solid symbols are measured on the E57Q mutant. The table in the supporting information gives the $^{15}N$ and NH chemical shifts of wild type MutT, its E57Q mutant, and their binary $Mg^{2+}$ and dGTP complexes.

Figure 3A,B, which compares typical $^{15}N$ planes of 3D $^{1}H-^{15}N$ NOESY-HSQC spectra of the wild type and E57Q mutant enzymes, shows that most of NOE cross-peaks of the wild type enzyme remain in the E57Q mutant. Even for the backbone NH of Gln-57 (inset), the NOE cross-peaks are very similar to those of the wild type enzyme. Actually, 85.6% (988 NOE's) of the NOE cross-peaks to the backbone NH resonances in the E57Q mutant are unshifted (i.e., <0.05 ppm), and show similar intensities to those of the wild type enzyme. Therefore, the overall three-dimensional fold of the E57Q mutant is very similar to that of the wild type enzyme.[2]

In addition, the 3D $^{1}H-^{15}N$ NOESY and TOCSY-HSQC spectra of both the wild type and the E57Q mutant showed very similar patterns and normalized intensities of exchange cross-peaks between the water resonance and backbone and side chain NH resonances (not shown). Most of the side chain $NH_2$ protons of Asn and Gln residues showed significant cross-peaks with water in both the mutant and wild type enzymes except those of the $N_\delta H_2$ of Asn-119, the $N_\epsilon H_2$ of Gln-55, and Gln-57, the mutated residue, indicating slow exchange with water protons.

The slow exchange rates of the side chain $NH_2$ protons of Gln-55, Gln-57, and Asn-119, in the E57Q mutant were confirmed in a transfer of saturation experiment which showed the smallest effects on their $NH_2$ resonances (Figure 4). Because all side chains of Asn and Gln residues are exposed, the slow exchange rate of Gln-57 probably arises from hydrogen bonding interactions. NOE cross-peaks from the side chain $NH_2$ resonances of Gln-57 to the $H_\beta$ and $H_\gamma$ resonances of Glu-98 indicate proximity and suggest that Gln-57 is hydrogen bonded to Glu-98. Proximity between Glu-57 and Glu-98 is also seen in the tertiary structure of the wild type enzyme (Figure 1).

[2] A preliminary determination of the solution tertiary structure of the E57Q mutant based on 1367 NOE's shows an overall fold very similar to that of the wild type enzyme.

While the overall tertiary fold is preserved in the E57Q mutant, selective changes in $^{15}N$ and NH chemical shifts in the $^{1}H-^{15}N$ HSQC spectrum are seen (Figure 2) which may result from the loss of negative charge at residue 57 or from a localized conformational change. The latter is suggested by changes in the intensities of several NOE's in the environment of residue 57 in the mutant. Thus the NOE from Pro-36 $H_{\beta 1,2}$ to the NH of Gly-37 changed from medium to weak, the NOE from Lys-39 NH to Ile-40 NH changed from weak to absent, and the NOE from Ile-6 $H_{\gamma 1}$ to Ala-7 NH changed from weak to medium.[2] Figure 5 (upper) summarizes regions of the backbone with significantly altered NH or $^{15}N$ chemical shifts, and Figure 6A locates these regions in the tertiary structure of the wild type enzyme. Backbone amides which experience significant changes in chemical shifts are residues 20 and 22 of $\beta$-strand B, 29, 38, and 49 of loop I, 57−59 of helix I, 60 and 64 of loop II, and 96−100 of loop III, comprising a large region which surrounds the site of the mutation (Figures 1 and 6A). Interestingly, the binding of $Mg^{2+}$ causes $^{15}N$ and NH chemical shift changes in these same regions of both the wild type and mutant enzymes, (see Figures 5 and 6A,B and below) indicating that charge neutralization by either $Mg^{2+}$ binding or the E57Q mutation produce similar effects.

*Binary $Mn^{2+}$ Complex of the E57Q Mutant Compared with That of the Wild Type Enzyme.* The binding of $Mn^{2+}$ to the E57Q mutant was studied by EPR and by $1/T_1$ of water protons. A Scatchard plot based on the EPR data (Figure 7) shows that the E57Q mutant binds $Mn^{2+}$ at $0.88 \pm 0.15$ sites with a dissociation constant, $K_2$, of $473 \pm 70$ $\mu$M. The binding affinity of $Mn^{2+}$ for the E57Q mutant is ~3.6-fold weaker than for the wild type enzyme ($K_2 = 130 \pm 40$ $\mu$M; Frick *et al.*, 1994) (Table 1). The binding of $Mn^{2+}$ to the E57Q mutant of MutT enhanced its paramagnetic effect on $1/T_1$ of water protons by a factor ($\epsilon_b$) of $8 \pm 2$, which is half of that found for the wild type enzyme ($\epsilon_b = 17 \pm 4$; Frick

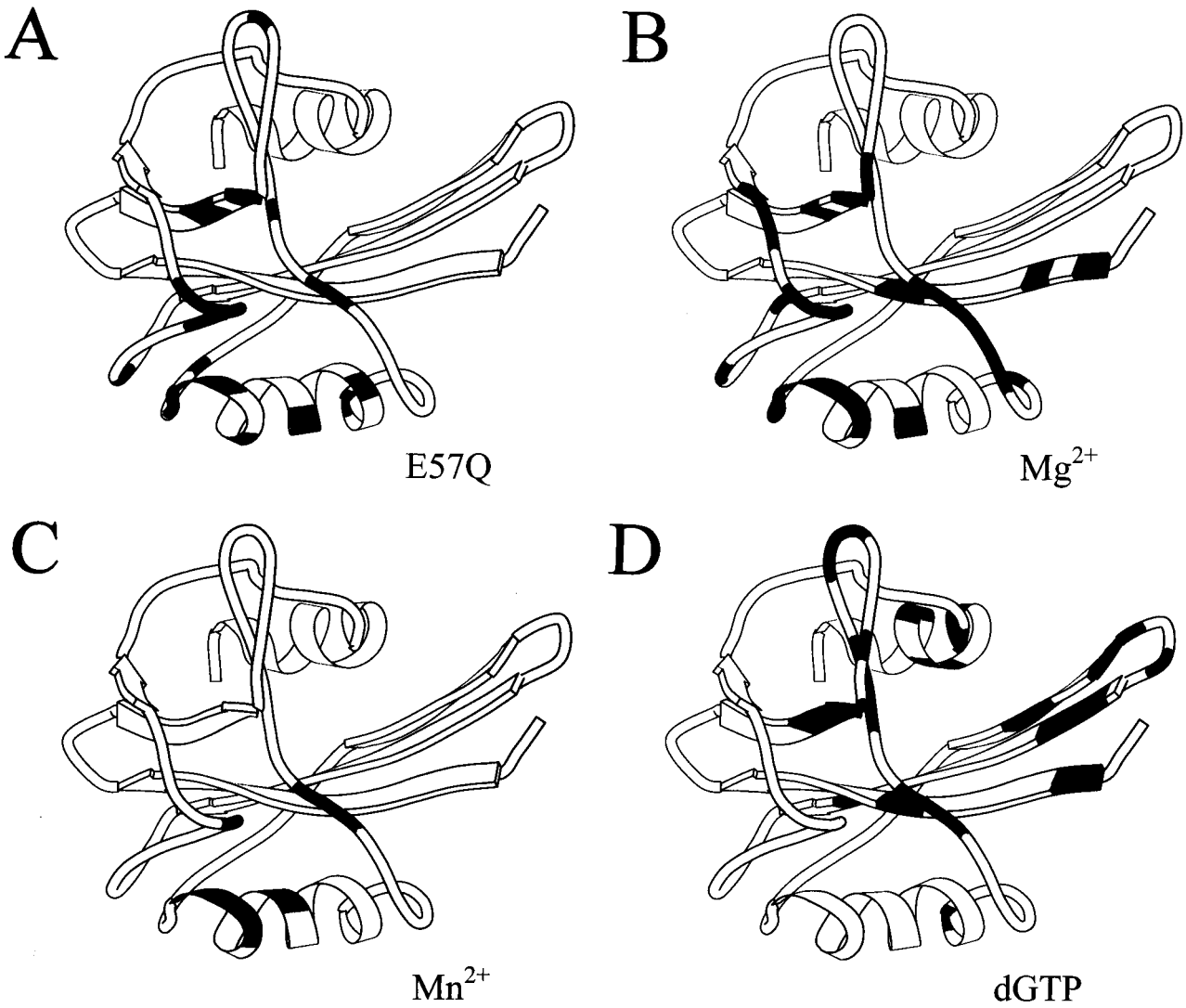


FIGURE 6: Regions of the MutT enzyme affected by (A) the E57Q mutation; (B) $Mg^{2+}$ binding; (C) $Mn^{2+}$ binding; (D) dGTP binding. A, B, and D indicate sites of $^{15}N$ and/or NH chemical shift changes in $^{1}H-^{15}N$ HSQC spectra. C indicates sites of distance-dependent resonance disappearance in $^{1}H-^{15}N$ HSQC spectra induced by $Mn^{2+}$ binding.

*et al*., 1994) indicating a major change in the coordination sphere of enzyme-bound $Mn^{2+}$ in the mutant.

*$^{1}H-^{15}N$ HSQC Titration of the Wild Type or E57Q Mutant Enzyme with $MnCl_2$.* To determine which residues are near the metal binding site and might function as ligands, the wild type enzyme (0.75 mM) was titrated with $MnCl_2$, monitoring the paramagnetic effects of $Mn^{2+}$ on the relaxation rates of the backbone NH resonances by $^{1}H-^{15}N$ HSQC spectra. In the presence of 6 $\mu$M $MnCl_2$ (Figure 8A), the backbone NH resonances of Gly-38 and Lys-39 in loop I almost disappeared, while the intensities of the resonances of Gly-37 in loop I and of Glu-53, Glu-56, Glu-57, and Val-58 in helix I decreased by 20%−60%. No broadening of the residual cross-peaks was observed. The mechanism of this paramagnetic effect is selective shortening by $Mn^{2+}$ of the transverse ($T_2$) and longitudinal ($T_1$) relaxation times of the $^{1}H$ and $^{15}N$ resonances. Shortening of $T_2$ results in decreased cross-peaks intensity because the INEPT and reverse INEPT transfer steps of the HSQC experiment selectively filter out broadened resonances. Shortening of $T_1$ by $Mn^{2+}$ decouples the $^{15}N-^{1}H$ interaction responsible for the cross-peaks, thereby decreasing their intensities. The extent of attenuation of a given cross-peak thus provides a phenomenological measure of the proximity of $Mn^{2+}$ to each $^{15}N-^{1}H$ vector. Smaller effects were noted on the backbone NH resonance of Glu-98 in loop III, which became much more pronounced at 9 $\mu$M $MnCl_2$. Figures 5, 6C, and 9A, which summarize the major effects, indicate that $Mn^{2+}$ binds to the free enzyme near loop I, helix I, and loop III.

On the basis of the magnitudes of these selective effects on $T_1$ and $T_2$ of the NH and/or $^{15}N$ resonances, possible ligands for enzyme-bound $Mn^{2+}$ are the carboxylate groups of Glu-57, Glu-53, and, less likely, those of Glu-56 and Glu-98. The backbone carbonyl groups of Lys-39, Gly-38, and, less likely, Gly-37 may also be ligands. Consistent with these suggestions, the solution structure of the free MutT enzyme (Figure 1) reveals short inter-oxygen distances, ranging from 3.4 to 6.8 Å, between the carboxylate groups of Glu-57, Glu-53, and the backbone carbonyl groups of Gly-37 and Lys-39. Somewhat longer inter-oxygen distances from the carboxylate of Glu-57 to those of Glu-56 (8.0−10.3 Å) and Glu-98 (8.3−9.0 Å) and to the backbone carbonyl group of Gly-38 (7.4 Å) are found. The coordination of $Mn^{2+}$ in an octahedral complex would decrease the inter-oxygen distances of its ligands to values of 3.1 and 4.4 Å for *cis* and *trans* ligands, respectively.

HSQC titration of the E57Q mutant with $MnCl_2$ shows a pattern of disappearance of NH and $^{15}N$ cross-peaks similar to that of the wild type enzyme (Figures 5 and 8A,B). Major effects again were observed on loop I centering around Lys-

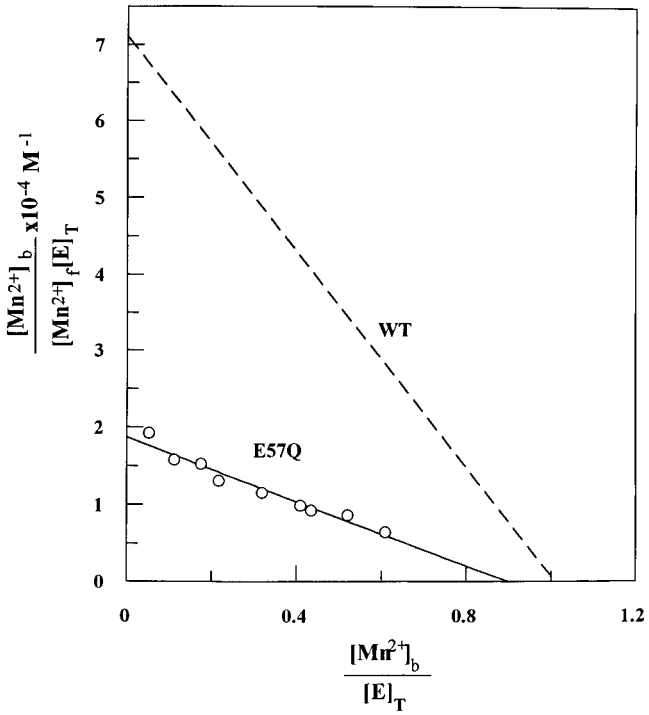


FIGURE 7: Scatchard plot of $Mn^{2+}$ binding by the E57Q mutant of MutT. Conditions are given in Materials and Methods. Also shown by the dashed line is the Scatchard plot for the wild type enzyme under identical conditions (Frick *et al*., 1994).

Table 1: Dissociation Constants ($\mu$M) of $Mg^{2+}$, $Mn^{2+}$, and dGTP Complexes of the Wild Type and the E57Q Mutant MutT Enzymes

| parameter | definition[a] | E57Q | wild type |
|---|---|---|---|
| $K_1$ | [E][G]/[EG] | 3420 ± 360[b] | 3440 ± 280[b] |
| $K_2$ | [E][Mn]/[EMn] | 470 ± 70[c] | 130 ± 40[c,d] |
| $K_2$ | [E][Mg]/[EMg] | 4850 ± 570[e] | 1450 ± 230[e] |
| $K_6$ | [EMg][GMg]/[EMgGMg] | 1760 ± 260 | |
| $K_{11}$ | [Mg][EGMg]/[EMgGMg] | 1350 ± 150[f] | |
| $K_{12}$ | [E][GMg]/[EGMg] | 6520 ± 690[f] | |

[a] G refers to dGTP. [b] Determined by $^1H-^{15}N$ HSQC titration of enzyme with dGTP. [c] Determined by EPR titration of enzyme with $MnCl_2$. [d] From Frick *et al*. (1994). [e] Determined by $^1H-^{15}N$ HSQC titration of enzyme with $MgCl_2$. [f] Determined by $^1H-^{15}N$ HSQC titration of E-$Mg^{2+}$ with $Mg^{2+}$-dGTP and calculated as described in Materials and Methods.

39 and on helix I centering around Gln- 57. The smaller effects of $Mn^{2+}$ on the E57Q mutant compared to those on the wild type enzyme, despite a 2-fold greater occupancy of the $Mn^{2+}$-binding site on the mutant enzyme (Figure 8), further indicate a change in the interaction of the bound metal ion with its ligands consistent with the decreased paramagnetic effect of $Mn^{2+}$ on water protons (see above). The largest paramagnetic effects of $Mn^{2+}$ on the E57Q mutant are on the amide side chain $NH_2$ signals of Gln-57 and the backbone NH of Lys-39 (Figure 9B), indicating that $Mn^{2+}$ binds nearest to these positions. Somewhat smaller effects occur on the backbone NH resonances of Gln-57, Glu-53, Glu-56, and Glu-98. The location of the $Mn^{2+}$ binding site on the E57Q mutant is therefore similar to that on the wild type. However it is not identical, since significantly smaller *relative* paramagnetic effects (i.e., relative to the largest effect on Lys-39) on the backbone NH resonances of Gly-37, Gly-38, Val-58, and Glu-98 are seen with the E57Q mutant than with the wild type enzyme (Figures 8 and 9). Hence a small movement of bound $Mn^{2+}$ away from these residues has occurred in the mutant.

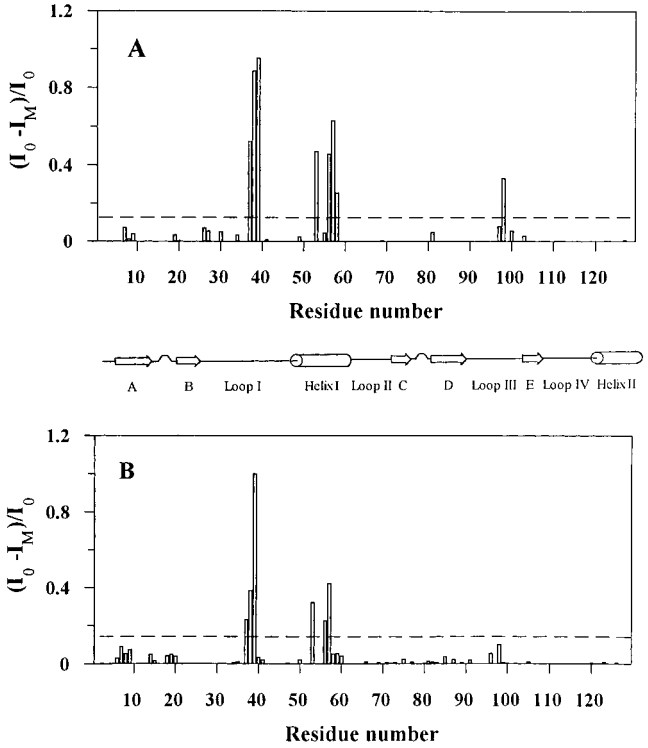


FIGURE 8: Comparison of the paramagnetic effects of $Mn^{2+}$ on the backbone NH signals in $^1H-^{15}N$ HSQC spectra of the wild type and E57Q mutant enzymes. The relative loss of peak intensity of the backbone NH in the HSQC spectra at a $Mn^{2+}$ concentration of 6 $\mu$M (wild type) or 16 $\mu$M (E57Q) was plotted against the residue number and secondary structure. $I_0$ is the peak intensity at 0 $Mn^{2+}$ concentration, and $I_M$ is the peak intensity at 6 $\mu$M $Mn^{2+}$ (wild type) or 16 $\mu$M $Mn^{2+}$ (E57Q mutant). (A) Wild type enzyme; [enzyme-bound $Mn^{2+}$] = 5.1 $\mu$M. (B) E57Q mutant enzyme; [enzyme-bound $Mn^{2+}$] = 9.8 $\mu$M. The dashed lines indicate the error limits.

*$^1H-^{15}N$ HSQC Titration of the Wild Type or the E57Q Mutant Enzyme with $MgCl_2$.* The binding of $Mg^{2+}$ to MutT was monitored by $^1H-^{15}N$ HSQC spectra in titrations of the E57Q mutant and wild type enzymes with $MgCl_2$. Changes in chemical shift were plotted against the concentration of $Mg^{2+}$ for those cross-peaks which showed the largest shifts ($\Delta\delta$ > 0.10 ppm for NH, $\Delta\delta$ > 0.40 ppm for $^{15}N$) and the data were fitted to eq 1 to obtain the dissociation constants ($K_2$) of the binary enzyme-$Mg^{2+}$ complexes and the chemical shift changes at saturating $Mg^{2+}$ ($\Delta\delta^\infty$) (Figure 10A). The average $K_2$ values obtained from five fits for the wild type enzyme and from eight fits for the E57Q mutant enzyme were used to evaluate the respective $\Delta\delta^\infty$ values for all of the NH and $^{15}N$ cross-peaks by extrapolation. Figure 10B,C gives the weighted sums of the effects on both the $^{15}N$ and NH chemical shifts. The separate effects on the $^{15}N$ and NH chemical shifts are given in Figures S-1 and S-2 of the supporting information. The $K_2$ values (Table 1) indicate that the binding of $Mg^{2+}$ to the E57Q mutant is 3.3-fold weaker than to the wild type enzyme. While the NH and $^{15}N$ chemical shifts of many of the same residues of the mutant and wild type enzymes changed in response to $Mg^{2+}$ binding, the $\Delta\delta^\infty$ values of the mutant were significantly smaller. Figures 5 and 6 summarize the effects of $Mg^{2+}$ and $Mn^{2+}$ binding and of the E57Q mutation itself on the $^1H-^{15}N$ HSQC spectra of the MutT enzyme.

The largest chemical shift changes induced by $Mg^{2+}$ binding were observed in backbone NH resonances of loop III from residues 95 to 100, in helix I from residues 53 to

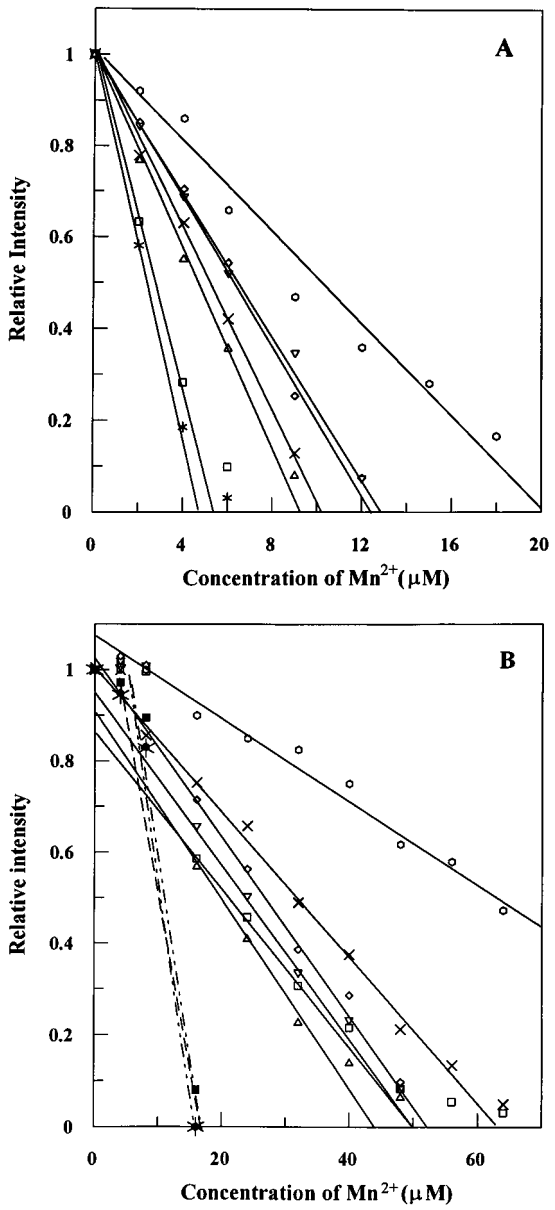


FIGURE 9: Comparison of the major paramagnetic effects versus the concentration of $Mn^{2+}$ on the backbone NH signals in $^1H-^{15}N$ HSQC spectra of the wild type and E57Q mutant enzymes. The relative peak intensities of the backbone NH signals in the HSQC spectra were plotted against the concentration of $Mn^{2+}$. The intensity of each peak was normalized using the C-terminal NH signal, which is unaffected by $Mn^{2+}$, as reference. (A) Wild type enzyme [G37 (×), G38 (□), K39 (*), E53 (▽), E56 (◇), E57 (△), E98 (○)]. (B) E57Q mutant enzyme [G37 (×), G38 (□), K39 (*), E53 (▽), E56 (◇), Q57 (△), E98 (○), Q57 side chain NH-1 (●), Q57 side chain NH-2 (■)].

59, and to a lesser extent in loop I (Figure 6B). Helix I and loop I are near the $Mn^{2+}$ binding site based on distance-dependent paramagnetic effects on the HSQC spectra (Figures 5 and 6B,C). Therefore, changes in chemical shifts of residues in this region represent both local and remote effects of $Mg^{2+}$ binding.

*Binary dGTP Complexes of the Wild Type and E57Q Mutant Enzymes.* $^1H-^{15}N$ HSQC titrations of the wild type and E57Q mutant enzymes with dGTP, the best substrate among the canonical nucleotides (Frick *et al*., 1995b), yielded identical dissociation constants (Figure 11A, Table 1) and very similar effects on the $^{15}N$ and NH chemical shifts for both proteins. Figure 11B,C gives the weighted sums of the effects on both the $^{15}N$ and NH chemical shifts. The separate effects on the $^{15}N$ and NH chemical shifts are given in Figures S-3 and S-4 of the supporting information. As summarized in Figures 5 and 6D, significant changes in chemical shifts on nucleotide binding were observed on $\beta$-strand A, centering around Val-8, on $\beta$-strand B, throughout loop I, on $\beta$-strand C and D, at the end of loop IV, and the beginning of helix II, especially Asn-119. From the three-dimensional structure of the free MutT enzyme (Figures 1 and 6D), these regions form the walls of a cleft defined by the three $\beta$-strands A, C, and D on one side and loop I, the end of loop IV, and the beginning of helix II, on the other side. Residues 37−39 of loop I are in contact with residues 7 and 8 of $\beta$-strand A, and Asn-119 (which is followed by helix II) is near the three $\beta$-strands. The observed changes in chemical shift upon binding of dGTP suggest the involvement of this cleft in substrate binding. Residues in loop III and helix I, which were affected by metal binding, did not show significant changes in chemical shifts on dGTP binding. On the other hand, loop I is affected by both metal and substrate binding (Figures 5 and 6).

In contrast to the large and widespread effects of dGTP on the $^1H-^{15}N$ HSQC spectrum of the wild type enzyme (Figure 11B), the binding of AMPCPP to the wild type enzyme showed much smaller effects on the resonances of $\beta$-strand A and little or no effects on those of $\beta$-strands C and D and loop IV (not shown). These differences are consistent with the substrate specificity of the MutT enzyme which shows a 50-fold greater $k_{cat}$ and a 4.2-fold smaller $K_m$ with dGTP in comparison with ATP (Frick *et al*., 1995b).

*Ternary Enzyme-Nucleotide-$Mg^{2+}$ and Quaternary Enzyme-$Mg^{2+}$-Nucleotide-$Mg^{2+}$ Complexes of the E57Q Mutant or Wild Type Enzyme.* $^1H-^{15}N$ HSQC titration of the E57Q mutant (0.75 mM) and $Mg^{2+}$ (6.0 mM) with $Mg^{2+}$-dGTP showed a similar pattern of effects as those of dGTP itself on the $^{15}N$ and NH chemical shifts of the mutant enzyme (Figure 5), indicating that the binding site of $Mg^{2+}$-dGTP on the enzyme-$Mg^{2+}$ complex is similar to that of dGTP on the free enzyme. However, the affinity for the metal substrate in the quaternary complex is greater. Fitting of the titration data with eqs 5−10 as described in Materials and Methods yielded dissociation constants $K_6$, $K_{11}$, and $K_{12}$ for the higher complexes of the mutant (Table 1).

The enzyme-bound $Mg^{2+}$ lowered the dissociation constant of $Mg^{2+}$-dGTP from the E57Q mutant by a factor of 3.7, as seen by comparing $K_6$, the dissociation constant of the quaternary complex, with $K_{12}$, that of the ternary complex. With the wild type enzyme, such titrations with $Mg^{2+}$-dGTP could not be carried out because of the high catalytic activity. However a kinetic analysis under similar conditions (Frick *et al*., 1994) showed that the enzyme-bound $Mg^{2+}$ lowered the $K_m$ of $Mg^{2+}$-dGTP by a factor of 44. Assuming $K_m$ to approximate $K_D$ (Frick et al., 1994), this order of magnitude greater effect with the wild type enzyme suggests that the interaction of $Mg^{2+}$-dGTP with the enzyme-bound metal is significantly weakened on the E57Q mutant enzyme, possibly by distortion or interruption of the metal−phosphate interaction.

To avoid nucleotide hydrolysis, the $Mg^{2+}$ complexes of both the wild type and E57Q mutant enzymes were titrated with $Mg^{2+}$-AMPCPP. The observed chemical shift changes of the $^{15}N$ and NH resonances were generally similar for both the wild type and mutant enzymes (not shown) and were too small for the accurate determination of dissociation constants. The largest effect was on the backbone $^{15}N$

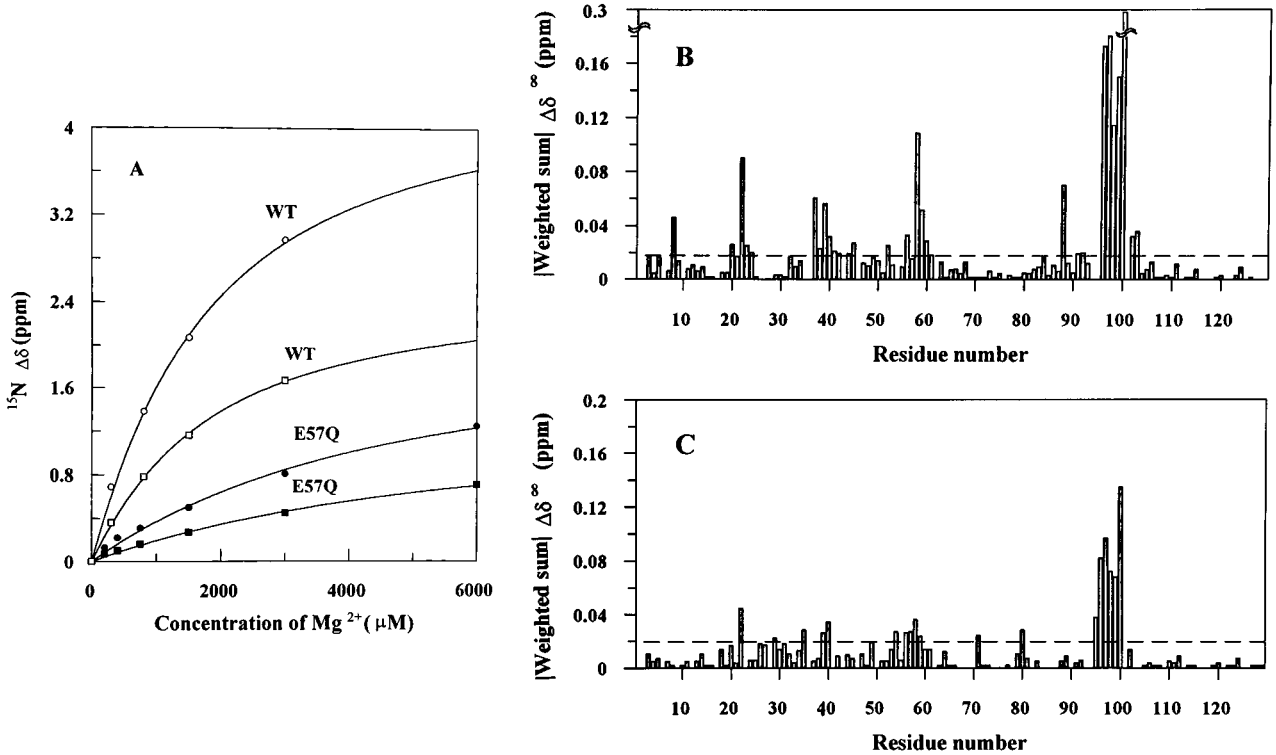


FIGURE 10: $^1$H−$^{15}$N HSQC titrations of the wild type and E57Q mutant enzymes with $MgCl_2$. (A) $MgCl_2$ was added to a solution containing 0.75 mM wild type or the E57Q mutant of MutT with the other components described in Materials and Methods, to final concentrations of 0.35, 0.75, 1.5, and 3.0 mM for the wild type and 0.2, 0.4, 0.75, 1.5, 3.0, and 6.0 mM for the E57Q mutant, respectively, and the HSQC spectra were recorded. Titration curves for the wild type and E57Q mutant are compared using the backbone $^{15}$N chemical shift changes of K97 [wild type (○), E57Q (●)] and Q100 [wild type (□), E57Q (■)], which are the resonances most sensitive to $Mg^{2+}$ binding. The curves fitted to the data were calculated using eq 1 and the dissociation constants ($K_2$) given in Table 1. B and C compare the effects of saturating [$Mg^{2+}$] on the weighted sums of the backbone $^{15}$N and NH chemical shifts of the wild type (B) and E57Q (C) enzymes. The weighted sums were calculated as in Figure 2. The individual effects on the $^1$H and $^{15}$N chemical shifts are given in Figures S-1 and S-2 and in the table in supporting information. The effects shown are the results of extrapolation to 1:1 complexes using the dissociation constants ($K_2$) given in Table 1. The dashed lines give the error limits.

chemical shift of Lys-97 which showed an 0.66 ppm upfield shift on the wild type enzyme and an insignificant 0.13 ppm downfield shift on the E57Q mutant (Figure 5). The resonance of Lys-97 (adjacent to Glu-98) is the one which is most affected by $Mg^{2+}$ binding, shifting by 4.6 ppm downfield on the wild type enzyme (Figure 10). The effects of the E57Q mutation are thus selective on the interaction of the enzyme-bound metal with the metal−nucleotide complex, since this mutation did not significantly alter the affinity or the chemical shifts induced by the binding of free dGTP to the free enzyme (Table 1, Figure 11A).

A comparison between the effects of $Mg^{2+}$-dGTP and $Mg^{2+}$-AMPCPP on the enzyme-$Mg^{2+}$ complex could be made only with the highly inhibited E57Q mutant. The $^{15}$N and NH chemical shifts produced by $Mg^{2+}$-AMPCPP are generally much smaller than those produced by $Mg^{2+}$-dGTP, and the effects of the adenine nucleotide on $\beta$-strands C and D and on the end of loop IV are negligible (Figure 5). Since the charges of $Mg^{2+}$-dGTP and $Mg^{2+}$-AMPCPP are identical, these differences could reflect conformational differences between the quaternary complexes of the two nucleotides. Conformational differences are consistent with the 50-fold greater $k_{cat}$ and 4.2-fold lower $K_m$ of dGTP over ATP as substrates of the wild type MutT enzyme (Bhatnagar & Bessman, 1988; Frick *et al.*, 1995b).

## DISCUSSION

Glutamate residues at the active site of the MutT enzyme (Figure 1) can, in principle, function either as metal ligands or as general bases to deprotonate the water which attacks the $\beta$-phosphorus of the NTP substrate. The side chain carboxylate of Glu-57 likely functions as a metal ligand for the enzyme-bound divalent cation as supported by four lines of evidence. First, the mutation of Glu-57 to Gln reduced the binding affinity of the enzyme for both $Mg^{2+}$ and $Mn^{2+}$ by 3.3−3.6-fold while the affinity for dGTP was essentially unaltered. Second, the E57Q mutation altered the ligand environment of enzyme-bound $Mn^{2+}$ as reflected in a 2-fold decrease in the enhancement of the paramagnetic effect on water proton relaxation and on nearby $^{15}$N−$^1$H vectors. Third, in the mutant, the side chain $NH_2$ of Gln-57 has the shortest distance to enzyme-bound $Mn^{2+}$ of all detectable NH signals with the exception of the backbone NH of Lys-39. At slightly greater distances are the backbone NH groups of Gln-57, Glu-53, Glu-56, and Glu-98 (Figure 9B). Fourth, the effects of the E57Q mutation itself on the NH and $^{15}$N chemical shifts of MutT are very similar to the effects of $Mg^{2+}$ binding on both the wild type and mutant enzymes (Figures 5 and 6A,B). Quantitation indicates that the sum of the effects of the E57Q mutation and of $Mg^{2+}$ binding to the mutant enzyme agrees with the effects of $Mg^{2+}$ binding to the wild type enzyme, suggesting that the loss of the negative charge at Glu-57, either by mutation or by neutralization with $Mg^{2+}$, is responsible for these effects. These

[3] The E57D mutant has recently been prepared, and preliminary studies indicate it to have significantly reduced but measurable activity. The pH dependence of this activity parallels that of the wild type enzyme, arguing against residue 57 functioning as a general base.

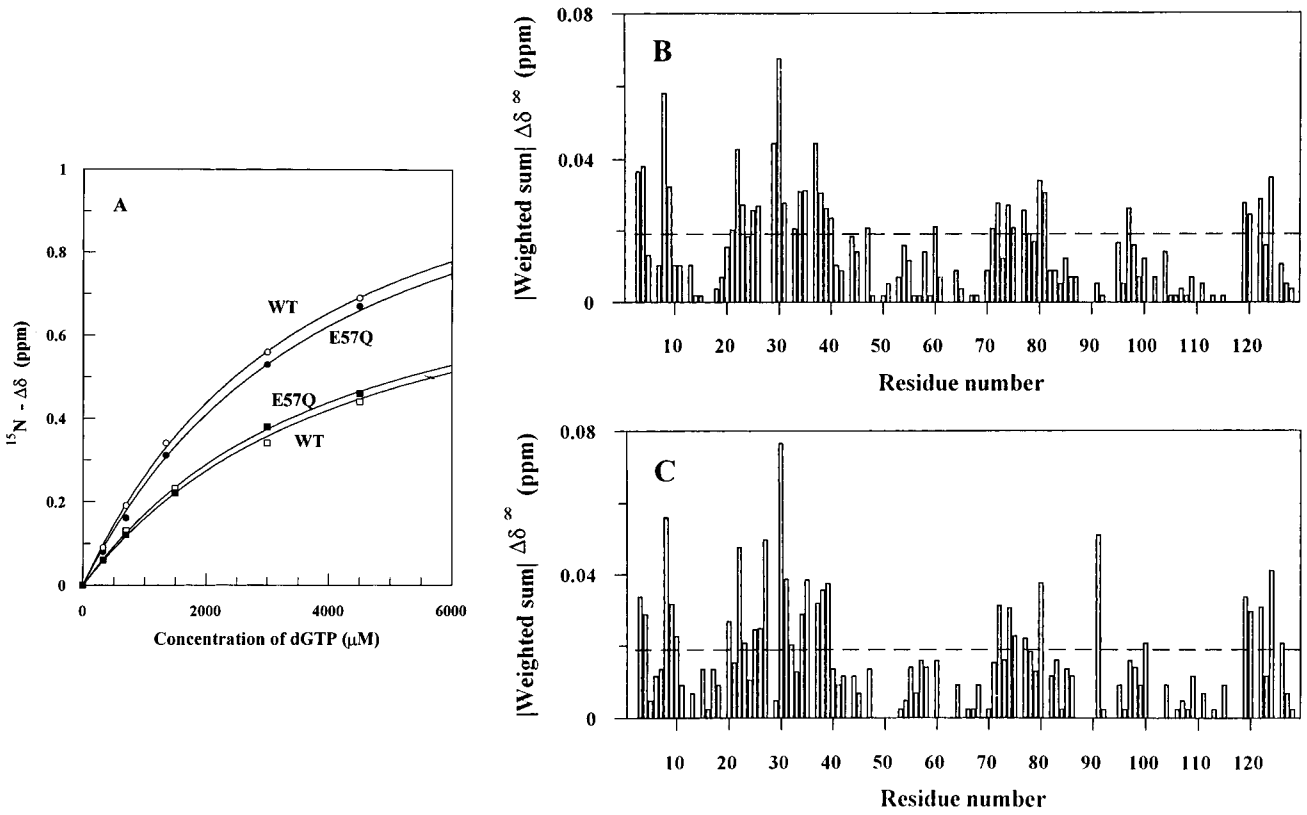


FIGURE 11: $^{1}$H−$^{15}$N HSQC titration of the wild type and E57Q mutant enzymes with dGTP. (A) dGTP was added to a solution containing 0.75 mM wild type or the E57Q mutant of MutT with the other components described in Materials and Methods to final concentrations of 0.35, 0.75, 1.5, 3.0, and 4.5 mM, and the HSQC spectra were recorded. Titration curves for the wild type and E57Q mutant were compared using the backbone $^{15}$N chemical shift changes of V8 [wild type (○), E57Q (●)] and E74 [wild type (□), E57Q (■)], which are the resonances most sensitive to dGTP binding. The curves were fitted to the data points using eq 1 and the dissociation constants ($K_1$) given in Table 1. B and C compare the effects of saturating dGTP on the weighted sums of the backbone $^{15}$N and NH chemical shifts of the wild type (B) and E57Q (C) enzymes. The weighted sums were calculated as in Figure 2. The individual effects on the $^{1}$H and $^{15}$N chemical shifts are given in Figures S-3 and S-4 and in the table in supporting information. The effects shown are the results of extrapolation to 1:1 complexes using the dissociation constants ($K_1$) given in Table 1. The dashed lines give the error limits.

results also suggest that in the $Mg^{2+}$ complex of the mutant enzyme, the side chain carbonyl oxygen of Gln-57 may function as a weak metal ligand.[3]

Although the global fold of the protein is preserved in the E57Q mutant, changes are found in the region of the mutation as shown by the chemical shift changes in the backbone $^{15}$N and NH resonances (Figures 5 and 6A). In the absence of the divalent cation, the change induced by the E57Q mutation may result from hydrogen bond donation by the side chain $NH_2$ of Gln-57 to nearby anionic residues such as Glu-98 and Glu-53. The effects of such an interaction on the protein conformation would be expected to mimic the effects of metal chelation by these residues. Such a model is supported by two observations. First, the side chain $NH_2$ protons of Gln-57 exchange more slowly with water than do those of any other other amide side chains (Figure 4) despite the fact that the solution structure of the free enzyme shows the side chain of Glu-57 to be exposed to solvent (Figure 1). Second, NOE cross-peaks from the side chain $H_\beta$, and $H_\gamma$ resonances of Glu-98 to the side chain $NH_2$ signals of Gln-57 are observed in the 3D $^{1}$H−$^{15}$N NOESY HSQC spectrum, indicating proximity of the two residues. Thus the replacement of a Glu (or Asp) residue by a Gln (or Asn) residue can provide a useful NMR probe of active site residues.

On the basis of the moderate affinity of the MutT enzyme for $Mn^{2+}$ ($K_D$ = 130 $\mu$M) and the high enhancement factor of the binary E-$Mn^{2+}$ complex, the enzyme likely donates a total of three or four ligands to the divalent cation, one of which is Glu-57. Other likely ligands to the enzyme-bound metal, suggested by the distance-dependent effects of $Mn^{2+}$ on both the wild type and mutant enzymes (Figure 9A,B) and by the solution structure of the free wild type enzyme (Figure 1), are the carboxylate side chain of the conserved residue, Glu-53, and the backbone carbonyl groups of Gly-38 and Lys-39. The carboxylate groups of the conserved residues Glu-98 and Glu-56 and the backbone carbonyl group of Gly-37, which are farther from the carboxylate of Glu-57 in the free enzyme, are therefore less likely ligands. However, they cannot be excluded. Another role of one of the conserved Glu residues at the active site is likely to be that of a general base.[3]

The profound ($\geq 10^5$-fold) decrease in catalytic activity of the E57Q mutant is unlikely to result solely from the weakening or loss of a metal ligand, since the complete loss of a ligand to $Ca^{2+}$ in the D40G mutant of staphylococcal nuclease similarly weakened $Ca^{2+}$ binding 3.3-fold but decreased $k_{cat}$ only 31-fold (Serpersu *et al.*, 1986). Clearly, structural and electronic changes at the metal binding site have occurred in the E57Q mutant of MutT. A change in the ligand field or a decrease in the number of water ligands on MutT-bound $Mn^{2+}$ is indicated by its decreased paramagnetic effect on water protons. If the water ligand which has been lost in the mutant is the attacking nucleophile in the MutT-catalyzed pyrophosphohydrolase reaction, then a major decrease in activity would result. A change in the precise location of the enzyme-bound metal in the mutant, indicated by the greater relative distance from $Mn^{2+}$ to Gly-37, Gly-38, Val-58, and Glu-98 (Figure 9) such that it

interacts less effectively with the metal-nucleotide substrate, may also contribute to the large decrease in activity. A 1.5 Å movement of $Ca^{2+}$ induced by the D21E mutation of staphylococcal nuclease decreased $k_{cat}$ by 1500-fold due to the direct coordination by $Ca^{2+}$ of Glu-43 in the mutant, making this catalytic residue unavailable to function as a general base or in orienting the attacking $OH^-$ ligand (Libson *et al*., 1994; Weber *et al*., 1994). Similarly, the loss of an anionic ligand to the metal in the E57Q mutant of MutT could result in the inappropriate coordination of the general base.

Electronic effects of altering the charge of a $Zn^{2+}$ ligand have been found with carbonic anhydrase where the mutation of the neutral His-94 ligand to an anionic Asp or Cys residue decreased $k_{cat}$ $\sim 10^2$-fold by raising the p$K_a$ of the attacking water ligand (Kiefer & Fierke, 1994). In the E57Q mutant of MutT, the replacement of an anionic ligand by an uncharged species would decrease the p$K_a$ of an attacking water ligand. When this water ligand has been deprotonated, the resulting metal-bound $OH^-$ would be less nucleophilic, inhibiting its attack on the electron-rich $\beta$-phosphorus of dGTP. Hence, both structural and electronic effects at the site of the enzyme-bound divalent cation are probably responsible for the major loss of activity of the E57Q mutant of MutT.[3]

The effects of dGTP binding on the $^1H-^{15}N$ HSQC spectra of both the wild type and E57Q mutant enzymes have been shown to be very similar (Figures 5 and 11). The backbone $^{15}N$ and NH chemical shifts altered by the binding of dGTP are located in a cleft in the solution structure of the wild type enzyme (Figures 1 and 6D). This cleft is formed by three $\beta$-strands (A, C, and D) on one side and loop I, the end of loop IV, and the beginning of helix II, on the other side. Several hydrophobic residues in the three $\beta$-strands have been found to be exposed to water and to point into the cleft, such as Tyr-73 and Phe-75 in $\beta$-strand C (Figure 1) (Abeygunawardana *et al*., 1995). Photoaffinity labeling of the MutT enzyme with 8-azido ATP followed by peptide mapping[4] has shown that a peptide consisting of residues 70−75 was labeled. Therefore, it is likely that the hydrophobic residues in these three $\beta$-strands, which are exposed to water, may be involved in substrate recognition by hydrophobic interactions. It is noteworthy that Phe-75 is conserved among MutT-like enzymes from all sources (Frick *et al*., 1995a). Asn-119, with its side chain pointing toward the three $\beta$-strands, may also be involved in substrate recognition, as suggested by the observation that the chemical shifts of not only the backbone NH (Figure 11B,C) but also the side chain $NH_2$ resonances of Asn-119 changed significantly on dGTP binding.

On the basis of these results, the active site of the MutT enzyme can be considered to consist of two subsites. One is the metal binding site, which is the reaction center of this enzyme, consisting of residues from loop I, helix I, and loop III (Figure 6C). The other is the nucleotide binding site, which determines the substrate specificity of the enzyme, and is formed by $\beta$-strands A, C, and D, loop I, and the end of loop IV near Asn-119 (Figure 6D). Unlike $Mg^{2+}$-dGTP, the binding of $Mg^{2+}$-AMPCPP to the enzyme-$Mg^{2+}$ complex caused relatively small changes in the chemical shifts of backbone NH resonances (Figure 5). These differences are consistent with the strong substrate preference of the MutT enzyme for guanine nucleotides over adenine nucleotides (Bhatnagar & Bessman, 1988).

[4] J. Lin and A. S. Mildvan, unpublished observations (1995).

## ACKNOWLEDGMENT

We are grateful to Dr. Apostolos G. Gittis for preparing Figure 1 and to Dr. Carol A. Fierke for helpful discussions.

## SUPPORTING INFORMATION AVAILABLE

Four figures, the separate effects of $Mg^{2+}$ on the $^{15}N$ and NH chemical shifts of wild type MutT (Figure S-1) and the E57Q mutant (Figure S-2) and those of dGTP on wild type MutT (Figure S-3) and the E57Q mutant (Figure S-4), and one table showing the $^{15}N$ and NH chemical shifts of wild type MutT, its E57Q mutant, and their binary $Mg^{2+}$ and dGTP complexes (11 pages). Ordering information is given on any current masthead page.

## REFERENCES

Abeygunawardana, C., Weber, D. J., Frick, D. N., Bessman, M. J., & Mildvan, A. S. (1993) *Biochemistry 32*, 13071−13080.
Abeygunawardana, C., Weber, D. J., Gittis, A. G., Frick, D. N., Lin, J., Miller, A.-F., Bessman, M. J., & Mildvan, A. S. (1995) *Biochemistry 35*, 14997−15005.
Bhatnagar, S. K., & Bessman, M. J. (1988) *J. Biol. Chem. 263*, 8953−8957.
Bhatnagar, S. K., Bullions, L. C., & Bessman, M. J. (1991) *J. Biol. Chem. 266*, 9050−9054.
Barik, S. (1993) *PCR Protocol: Current Methods and Applications* (White, B. A., Ed.) Vol. 15, pp 277−286, Humana Press Inc., Totowa, NJ.
Cheng, K. C., Cahill, D. S., Kasai, H., Nishimura, S., & Loeb, L. A. (1991) *J. Biol. Chem. 267*, 166−172.
Cohn, M., & Townsend, J. (1954) *Nature 173*, 1090−1091.
Frick, D. N., Weber, D. J., Gillespie, J. R., Bessman, M. J., & Mildvan, A. S. (1994) *J. Biol. Chem. 269*, 1794−1803.
Frick, D. N., Townsend, B. D., & Bessman, M. J. (1995a) *J. Biol. Chem. 270*, 24086−24091.
Frick, D. N., Weber, D. J., Abeygunawardana, C., Gittis, A. G., Bessman, M. J., & Mildvan, A. S. (1995b) *Biochemistry 34*, 5577−5586.
Kamath, A. V., & Yanofsky, C. (1993) *Gene 134*, 99−102.
Kiefer, L. L., & Fierke, C. A. (1994) *Biochemistry 33*, 15233−15240.
Kraulis, P. J. (1991) *J. Appl. Crystallogr. 24*, 946−950.
Levy, G. C., & Lichter, R. L. (1979) *Nitrogen-15 Nuclear Magnetic Resonance Spectroscopy*, John Wiley & Sons, New York.
Libson, A. M., Gittis, A. G., & Lattman, E. E. (1994) *Biochemistry 33*, 8007−8016.
Lin, J., Abeygunawardana, C., Frick, D. N., Bessman, M. J., & Mildvan, A. S. (1996) Biophysical Society Meeting, Baltimore, MD, February 17−21, 1996, Abstract Su-Pos-163, *Biophys. J. 70*, A61.
Maki, H., & Sekiguchi, M. (1992) *Nature 355*, 273−275.
Mejean, V., Salles, C., Bullions, L. C., Bessman, M. J., & Claverys, J.-P. (1994) *Mol. Microbiol. 11*, 323−330.
Mo, J. Y., Maki, H., & Sekiguchi, M. (1992) *Proc. Natl. Acad. Sci. U.S.A. 89*, 11021−11025.
Mori, S., Abeygunawardana, C., Johnson, M. O., & van Zijl, P. C. M. (1995) *J. Magn. Reson. B108*, 94−98.
Sakumi, K., Furuichi, M., Tsuzuki, T., Kakuma, T., Kawahata, S., Maki, H., & Sekiguchi, M. (1993) *J. Biol. Chem. 268*, 23524−23530.
Sarkar, G., & Sommer, S. S. (1990) *BioTechniques 8*, 404−407.
Serpersu, E. H., Shortle, D., & Mildvan, A. S. (1986) *Biochemistry 25*, 68−77.
Weber, D. J., Bhatnagar, S. K., Bullions, L. C., Bessman, M. J., & Mildvan, A. S. (1992) *J. Biol. Chem. 267*, 16939−16942.
Weber, D. J., Abeygunawardana, C., Bessman, M. J., & Mildvan, A. S. (1993) *Biochemistry 32*, 13081−13088.
Weber, D. J., Libson, A. M., Gittis, A. G., Lebowitz, M. S., & Mildvan, A. S. (1994) *Biochemistry 33*, 8017−8028.
Zhang, O., Kay, L. E. Olivier, J. P., & Foreman-Kay, J. D. (1994) *J. Biomol. NMR 4*, 845−858.

BI953071X